frontiers | Frontiers in Earth Science

TYPE Original Research
PUBLISHED 06 July 2023
DOI 10.3389/feart.2023.1218215

OPEN ACCESS

EDITED BY
Ruyue Wang,
SINOPEC Petroleum Exploration and Production Research Institute, China

REVIEWED BY
Shuai Yin,
Xi'an Shiyou University, China
Mengdi Sun,
Northeast Petroleum University, China

*CORRESPONDENCE
Yuqiang Jiang,
xnsyjyq3055@126.com

RECEIVED 06 May 2023
ACCEPTED 26 June 2023
PUBLISHED 06 July 2023

CITATION
Fang R, Jiang Y, Sun S, Luo Y, Qi L, Dong D, Lai Q, Luo Y and Jiang Z (2023), Controlling factors of organic matter accumulation and lacustrine shale distribution in Lianggaoshan Formation, Sichuan Basin, SW China.
Front. Earth Sci. 11:1218215.
doi: 10.3389/feart.2023.1218215

Controlling factors of organic matter accumulation and lacustrine shale distribution in Lianggaoshan Formation, Sichuan Basin, SW China

Rui Fang[1,2], Yuqiang Jiang[1,2]*, Shasha Sun[3], Yao Luo[4], Lin Qi[5], Dazhong Dong[3], Qiang Lai[5], Yuzhuo Luo[6] and Zengzheng Jiang[7]

[1]School of Geosciences and Technology, Southwest Petroleum University, Chengdu, China, [2]The Unconventional Reservoir Evaluation Department, PetroChina Key Laboratory of Unconventional Oil and Gas Resources, Chengdu, China, [3]PetroChina Research Institute of Petroleum Exploration and Development, Beijing, China, [4]Southwest Geophysical Exploration Branch of China Petroleum Group Dongfang Geophysical Exploration Co., Ltd., Chengdu, China, [5]Geology Exploration and Development Research Institute, CNPC Chuanqing Drilling Engineering Co., Ltd., Chengdu, China, [6]Northeastern Sichuan Oil and Gas District, PetroChina Southwest Oil and Gas Field Company, Dazhou, China, [7]Sichuan Geotech Science and Technology Ltd., Company, Chengdu, China

The lacustrine shale, represented by the Lianggaoshan Formation, is widely distributed in oil and gas basins of China and will be a key target for unconventional hydrocarbon exploration in the future. Due to the complexity of geological conditions, the distribution of lacustrine shale and the mechanism of organic matter (OM) enrichment show significant differences between different basins. In this study, seismic interpretation, core observation, high-frequency geochemical analysis and other methods are integrated to reveal factors controlling lacustrine shale distribution and OM accumulation in lacustrine shale. The results suggest that six bottom-to-top organic-rich shale intervals are identified within the Lianggaoshan Formation due to lake-basin migration. The migration process of depocenters controls the planar distribution of lacustrine organic-rich shale. The organic-rich lacustrine shale within 1st Member and 2nd Member is characterized by relatively high paleoproductivity and dysoxic condition. The lacustrine organic-rich shale of the upper to the top of 3rd Member is characterized by relatively low paleoproductivity, relatively high terrestrial input, and dysoxic condition. Paleoproductivity and preservation condition caused by lake-level rise are generally the major influencing factor of organic matter accumulation in 1st Member and 2nd Member organic-rich shale. The input of terrestrial OM, and the condition of preservation caused by rapid deposition are the major factors controlling OM accumulation in 3rd Member of Lianggaoshan Formation.

KEYWORDS

Jurassic, lacustrine shale, lake-basin, organic matter enrichment, Lianggaoshan Formation, Sichuan Basin

Introduction

Organic matter (OM) in fine-grained sedimentary rock (such as shale) is not only an important carrier of reservoir space and hydrocarbon occurrence, but also the material basis for hydrocarbon formation (Ross and Bustin, 2009; Fu et al., 2019; Zou, 2019; Fu et al., 2021). Its content is closely related to oil and gas production in both conventional and unconventional reservoirs (Zou et al., 2013; Zou et al., 2019; Li et al., 2022; Li et al., 2023). The OM enrichment in fine-grained sedimentary rock has important guiding significance for the prediction and evaluation of hydrocarbon "sweet spots" (Qiu and Zou, 2020a; Qiu and Zou, 2020b). The OM enrichment in shale is a complex physical-chemical process, which is affected by paleoclimate condition, paleoredox condition, paleosalinity, regional tectonic background, sediment transport process, hydrothermal activity, volcanic activity, gravity flow deposition (Deng et al., 2019; Liang et al., 2020; Liu et al., 2020; Gu et al., 2022a; Gu et al., 2022b; Lei et al., 2023). The impact of various paleo-environmental factors such as major geological events (water hypoxia events, biological extinction events) (Murphy et al., 2000), and the mechanisms (favorable or unfavorable) of different environmental conditions affecting OM can be summarized into three types of elements: input, preservation, and dilution of OM. The OM input mainly includes net primary productivity of endogenous seawater (or lake water) (excluding respiratory consumption by producers themselves) and inflow of terrestrial OM accompanied by debris (Lei et al., 2023). The preservation of organic matter mainly refers to the amount of input OM remaining on the sediment surface (after degradation and before sedimentation), which is mainly related to the redox characteristics of bottom water (Tribovillard et al., 2006). Dilution of OM mainly refers to the dilution of the molar concentration of OM by the input amount and input rate (or authigenic carbonate yield) of terrestrial debris (Deng et al., 2019).

The successful development of marine shale oil benefits by countries represented by the United States has triggered a wave of unconventional hydrocarbon exploration and development worldwide (Wang et al., 2016a; Wang et al., 2016b; Wang et al., 2018; Jiang et al., 2022). In recent years, the practical experience of marine shale oil has been continuously applied to the geological studies of lacustrine shale hydrocarbon resources (Lu et al., 2012). Major breakthroughs in shale oil have been achieved in several sedimentary basins in western and northern China (Hu D. et al., 2021; Hu Z. et al., 2021; He et al., 2022; Cai et al., 2023; Lai et al., 2023).

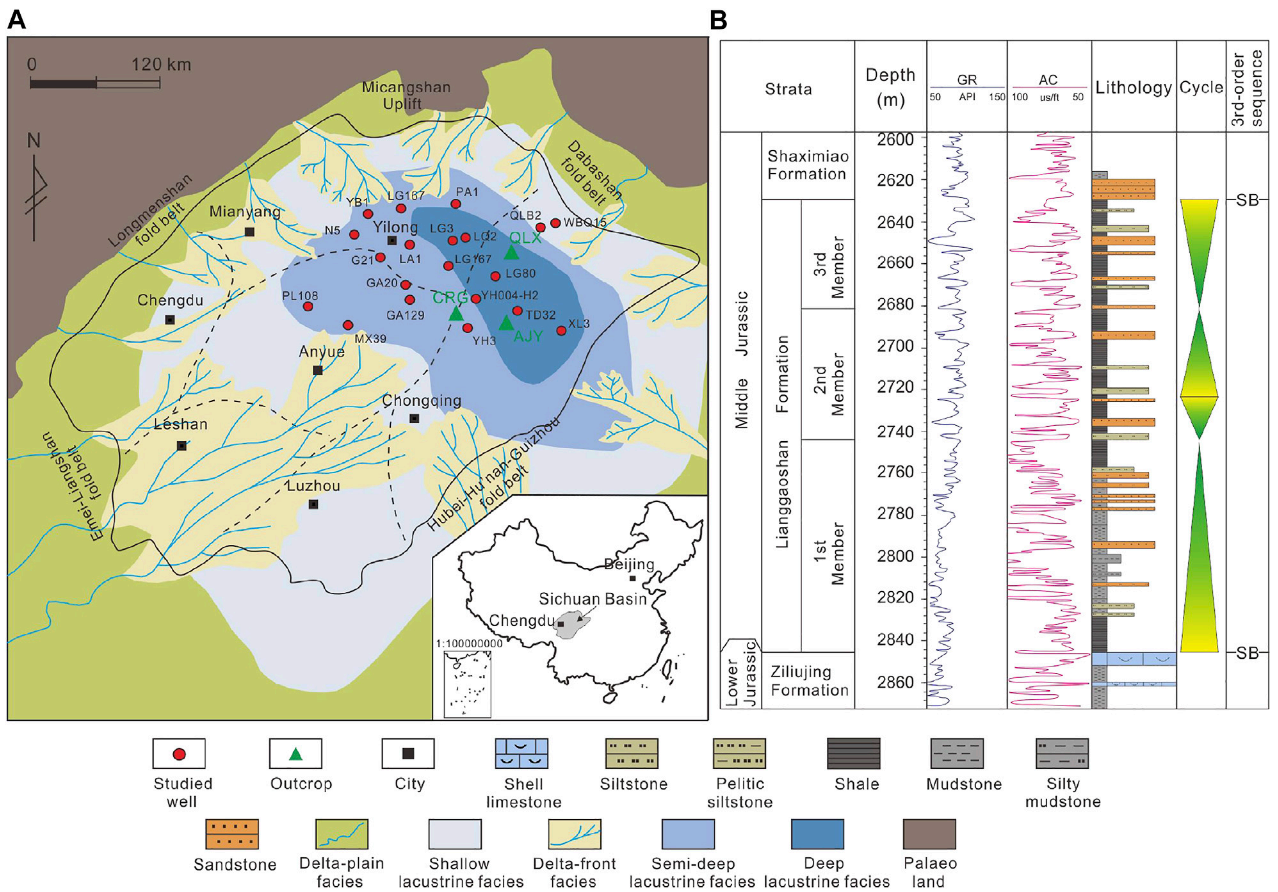

FIGURE 1
(A) Paleogeography of Lianggaoshan Fm. in Sichuan Basin. (B) Stratigraphic column of Jurassic Lianggaoshan Fm. in Sichuan Basin. SB, sequence boundary.

TABLE 1 Sedimentary facies division of Lianggaoshan Fm. in Sichuan Basin.

Facies	Subfacies	*In-situ* facies
Delta	Delta front	Underwater distributary channel
		Underwater natural levee
		Mouth bar
		Distal bar
	Delta plain	Natural levee
		Distributary channel
		Floodplain
Lake	Shallow lake	Shell shoal
		Sand bar
		Mud flat
	Semi-deep lake	Lacustrine mud

Breakthroughs have been obtained in the exploration of lacustrine shale hydrocarbons of the Middle Jurassic Lianggaoshan Fm. from Pingchang and Fuling areas of the Sichuan Basin since 2017 (Hu D. et al., 2021; Hu Z. et al., 2021; Cheng et al., 2023), demonstrating a good prospect for unconventional hydrocarbon exploration within the Lianggaoshan Formation. However, due to the significant differences in geological background between different basins and different environmental conditions during the development of lacustrine shale, there is significant uncertainty in its application, which poses great difficulties for exploration and development.

Based on seismic interpretation, core observation, high-frequency geochemical analysis and other methods, this study aims to reveal the lake-basin migration in the sedimentary process of Lianggaoshan Formation, characterizes the paleoenvironment of organic-rich shale, discusses the control of paleoclimate, redox properties of water bodies, paleoproductivity, and paleosalinity on organic matter enrichment, and reveals the relationship between the distribution of lacustrine shale, organic matter enrichment, and the sedimentary process of Lianggaoshan Formation.

Geological setting

The Sichuan Basin is located in southwestern China. During the sedimentary period of the Early Jurassic Ziliujing Formation (Fm.) to the Middle Jurassic Lianggaoshan Fm., the vast majority of this Basin belongs to the delta-lake sedimentary system (Figure 1A). The provenance of Lianggaoshan Fm., can be divided into three types: Type I, Type II and Type III, which reflects that the nature of parent rock has changed from igneous rock to metamorphic rock and sedimentary rock. The provenance areas correspond to the Micangshan area, northern margin of Yangtze plate, and Dabashan area respectively (Cheng et al., 2023). After the completion of Lianggaoshan Fm., sedimentation, the basin was converted into a river sedimentary system in internal conversion during the Middle Jurassic Shaximiao Fm., sedimentation period

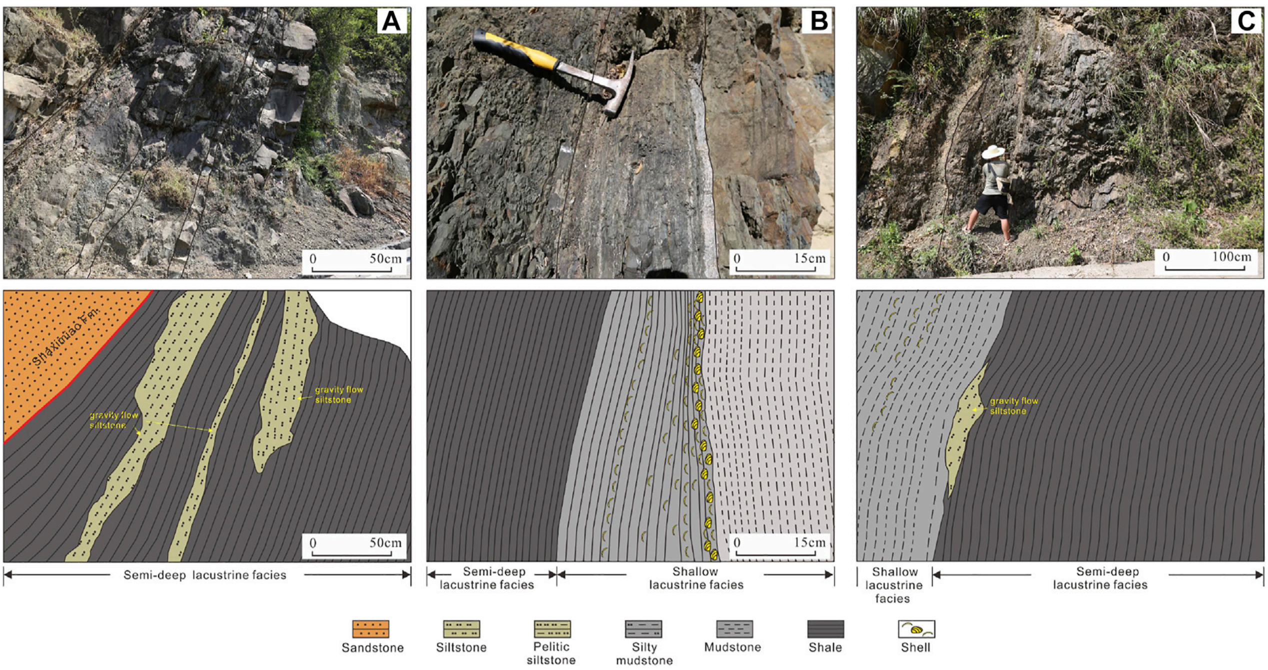

FIGURE 2
Typical lithological combinations and sedimentary facies types of Lianggaoshan Fm. in outcrops. **(A)** Gravity flow siltstone in black shale of semi-deep lake, QLX Outcrop, 3rd Member. **(B)** Black shale formed in semi-deep lake and grey mudstone formed in shallow lake, CRG Outcrop, 1st Member. **(C)** Shallow lacustrine grey mudstone and semi-deep lacustrine black shale, AJY Outcrop, 2nd Member.

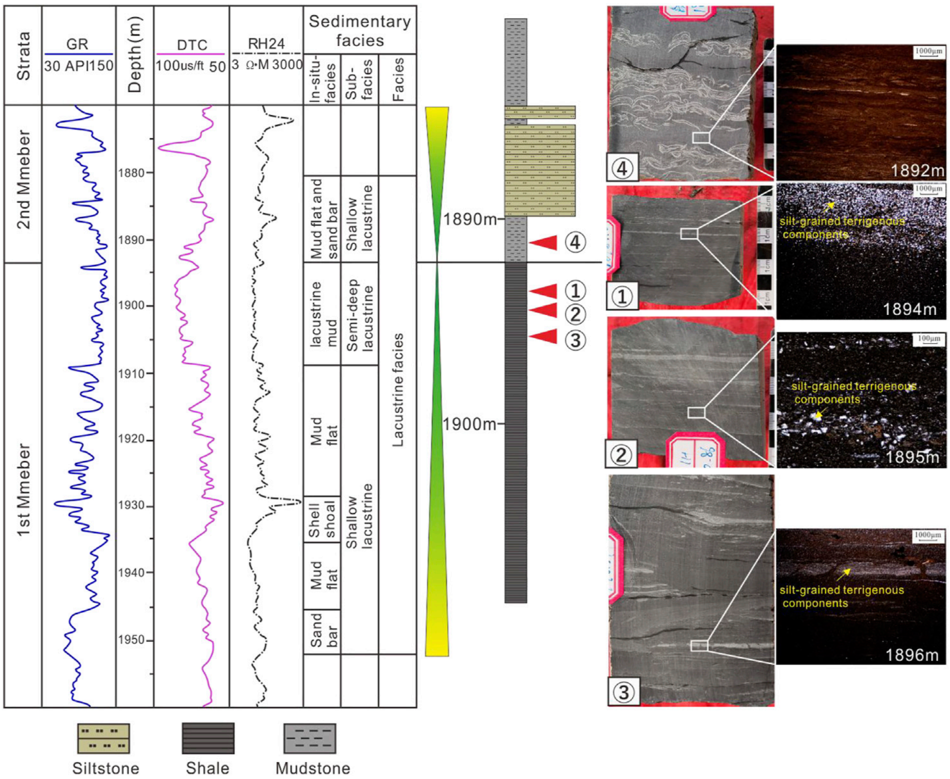

FIGURE 3
Development characteristics of lacustrine organic-rich shale in 1st Member of Lianggaoshan Fm., (based on Well HQ1).

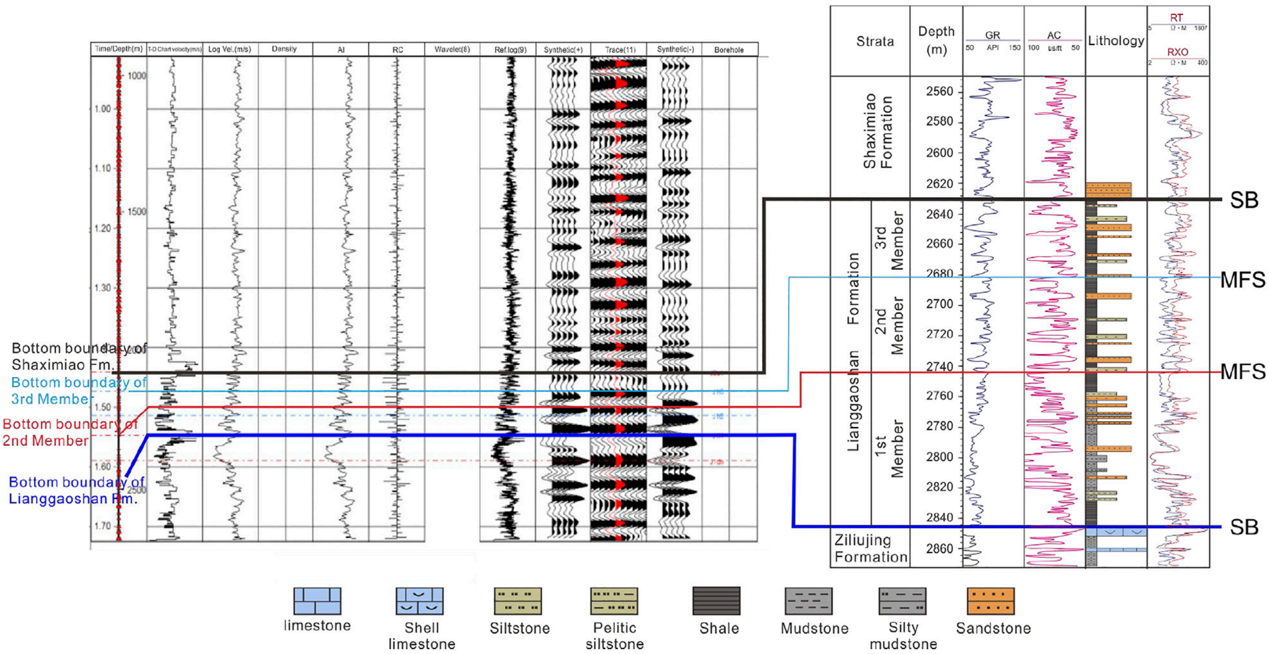

FIGURE 4
Synthetic seismogram of Jurassic system in Well LG3. MFS, maximum flooding surface; SB, sequence boundary.

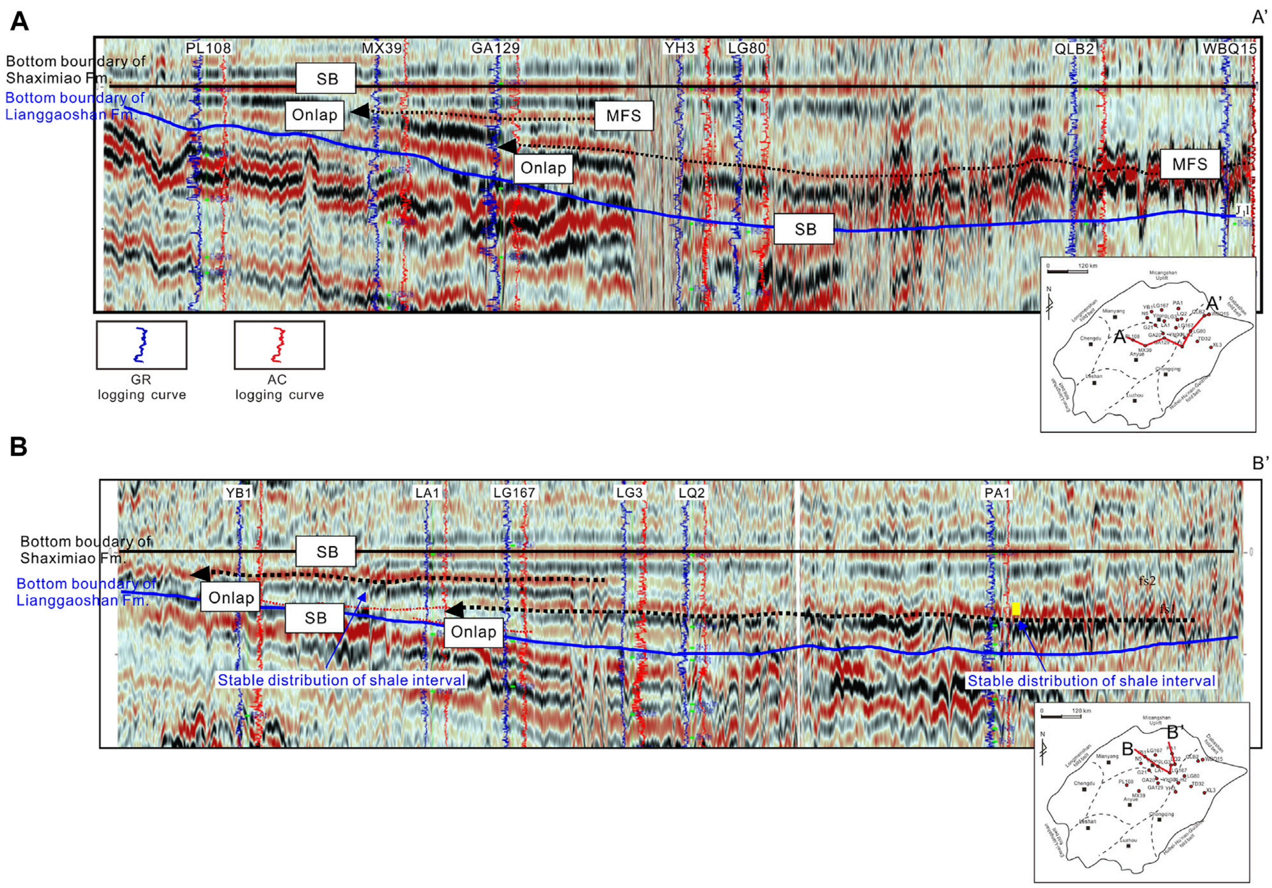

FIGURE 5
Seismic section showing maximum flooding surface (MFS) and sequence boundary (SB) in Lianggaoshan Formation. **(A)** Well PL108-MX39-GA129-YH3-LG80-QLB2-WBQ15. **(B)** Well YB1-LA1-LG167-LG3-LQ2-PA1.

(Cheng et al., 2023; Hu et al., 2023). The Lianggaoshan Fm., forms a separate third-order sequence, with a sequence boundary between the underlying and upper strata (Figure 1B). The Lianggaoshan Fm., belongs to the Middle Jurassic Aalenian to Bajocian Stage in terms of geological age (Huang, 2019), with a total thickness ranging from 100 to 260 m. The stratigraphic thickness gradually decreases from northeast to southwest. According to the characteristics of rock assemblages and cyclicity, the Lianggaoshan Fm., is divided into three segments: 1st Member, 2nd Member, and 3rd Member (Figure 1B).

Samples and methods

First, four Shaximiao Formation mudstone/shale samples and 28 Lianggaoshan shale samples obtained from coring wells were processed into 25 mm × 25 mm rock sample. Then, these rock samples were made into 0.03 mm thick thin-sections. Before the observation of petrology characteristics, the thin-sections shall be pretreated with mixed solution of alizarin red-S and potassium ferrocyanide.

The rock type and microscopic characteristics of thin-sections were observed through a Carl Zeiss polarizing microscope. The remaining samples were ground to 200 mesh powder by a mortar for elemental content detection. The main elements were tested using the Axios PW4400 X-ray fluorescence spectrometer, while the trace elements (TE) were tested using the Thermo X Series 2 plasma mass spectrometer. Corresponding analysis accuracy of both was below 5%. The TOC value was obtained using the American LECO CS-230 infrared sulfur and carbon analyzer, and pyrolysis parameters such as S_1, S_2, and T_{max} were obtained using the OGE-II rock pyrolysis analyzer.

Classification and characteristics of sedimentary facies

The main sedimentary facies types of Lianggaoshan Fm. include delta and lacustrine facies (Hu et al., 2023). The delta facies are mainly composed of delta front and delta plain subfacies (Cheng et al., 2023). The lake facies can be subdivided into shallow lake and semi-deep lake subfacies (Table 1). The semi-deep lake subfacies are mainly characterized by black shale (Figure 2A), and siltstone bodies of gravity flow origin are developed inside. The shallow lake subfacies are mainly characterized by gray mudstone (Figure 2B), and shell fossils can be observed internally (Figures 2B, C). The delta

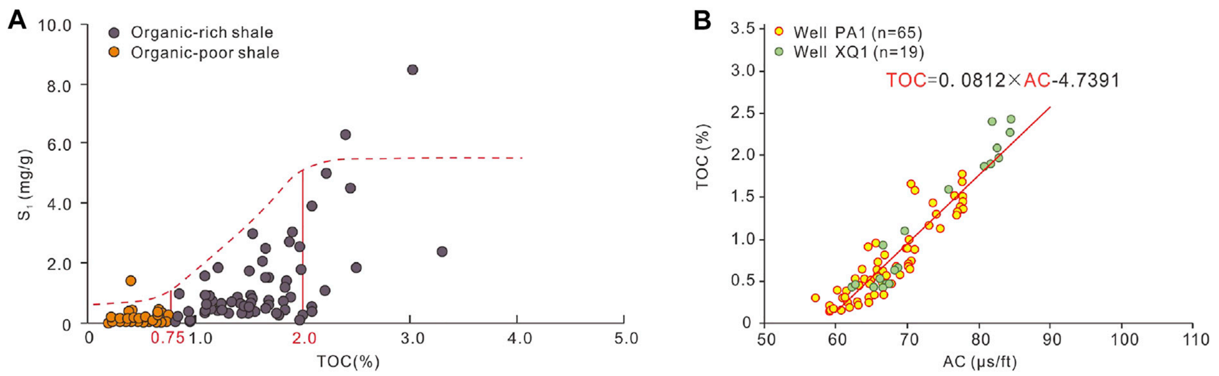

FIGURE 6
Correlations between different indicators. **(A)** TOC-S_1 diagram for Lianggaoshan lacustrine shale. **(B)** AC-TOC diagram for Lianggaoshan lacustrine shale.

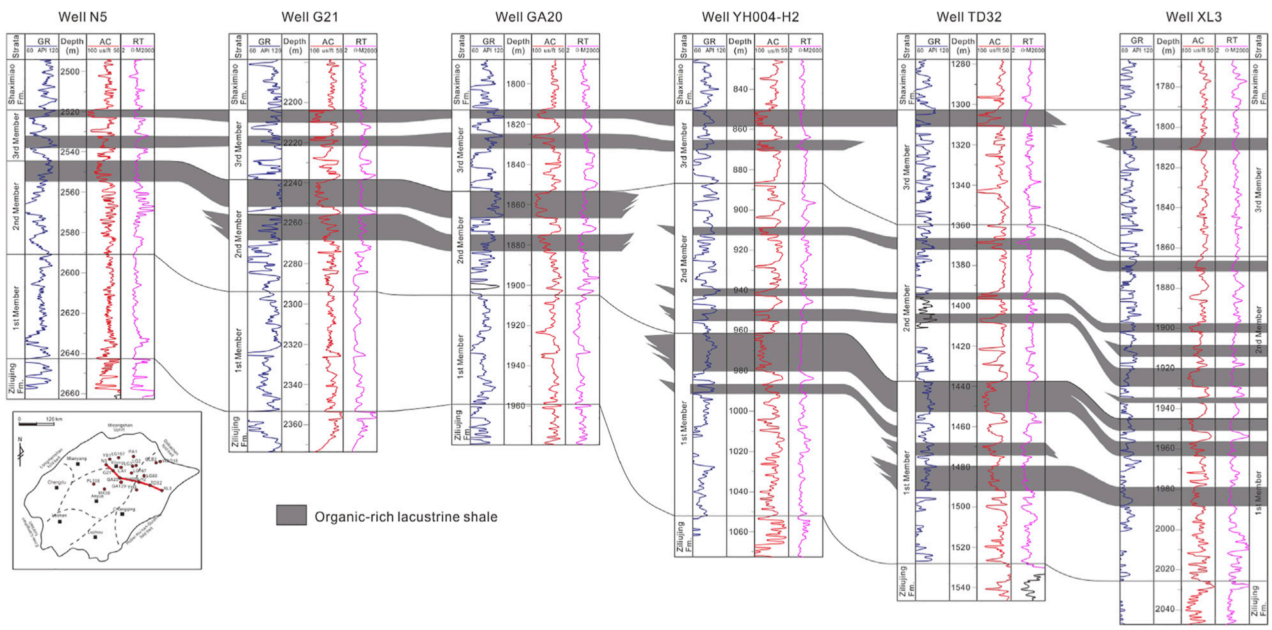

FIGURE 7
Cross-section showing distribution of Lianggaoshan organic-rich lacustrine shale.

facies does not affect the development of lacustrine shale, so this study will not discuss it.

Sedimentary evolution of lacustrine facies

Variation of lake level and sequence division

The frequent migration of continental lake-basins and the rise and fall of lake-levels make it difficult to apply traditional system tract classification methods due to the unclear system tract characteristics of lake-basin sequence stratigraphy (Cheng et al., 2023). Previous studies based on outcrop observation received that the Lianggaoshan lake-basin underwent a complete cycle of lacustrine transgression-lacustrine extension, which was divided into a 3rd-order sequence. Using seismic data, sequence boundary (SB) and maximum flooding surface (MFS) can be identified, which is easy to operate in the actual work of sequence stratigraphy and is convenient for analysis and research (Figure 4). Therefore, using the lacustrine transgression-lacustrine extension system tract division can more intuitively understand the evolution process of lake-basin and explain the filling pattern of sedimentary sequences.

During the sedimentary period of the Lianggaoshan Fm., the tectonic setting was relatively stable and it was a large depression

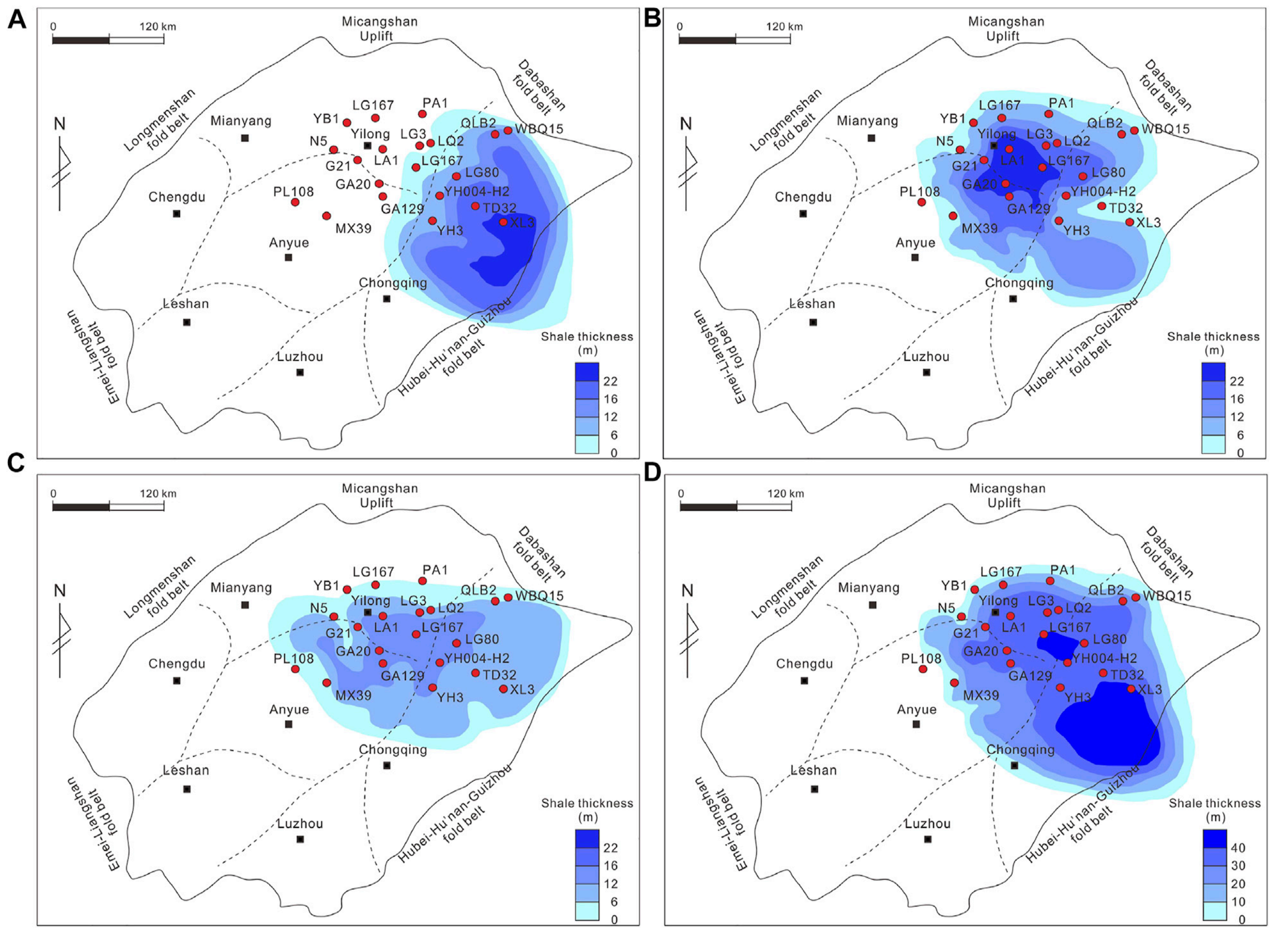

FIGURE 8
Contour plot showing distribution of Lianggaoshan lacustrine organic-rich shale. **(A)** Lianggaoshan 1st Member. **(B)** Lianggaoshan 2nd Member. **(C)** Lianggaoshan 3rd Member. **(D)** Lianggaoshan Formation.

lake-basin (Bai et al., 2022; Cheng et al., 2023). The top boundary of Lianggaoshan Fm. is bounded by black grey mudstone/shale and sandstone at the bottom of Shaximiao Formation. The logging curve features upward that GR changes from box high value to toothed medium low value, acoustic curve changes from high value to low value, and resistivity changes from box low value to toothed high value. This interface is a typical lithologic discontinuity (Figure 2A). The shale at the bottom of the Lianggaoshan Fm. is in integrated contact with the limestone of the underlying Ziliujing Fm., which is also a lithological discontinuous surface (Figure 1B). These two lithological mutation surfaces serve as 3rd-order sequence boundary (SB), and the division of sequence boundary in the Lianggaoshan Fm. is widely accepted and recognized, without controversy. Petrology characteristics of maximum flooding surface (MFS): it is located in the position where the maximum lake transgression reaches in the sequence, which is the boundary between lacustrine transgression system tract and extension system tract, and is characterized by retrogradation cycles (or parasequence sets) turning into progradation or aggradation cycles (or parasequence sets). The Lianggaoshan Fm. MFS is shown as the upper part of a large section of black shale on the core (Figure 3). This section of shale is characterized by deep color and laminated structure. The continuous thickness of the shale interval is 12–25 m, and pyrite grains can be seen, which reflects the sedimentary environment of strong reduction, and does not contain or have less scale debris (Figure 3). MFS in the study area is relatively easy to identify, mainly manifested as straight or toothed high GR, high acoustic time difference, and low electrical resistance characteristics (Figure 4). Among them, the acoustic time difference is affected by the lower velocity of black shale, and the high value of the box shaped is obvious.

Evolution and migration of lake-basin

This study uses the maximum flooding surface (MFS) and spatial distribution of shale/mudstone to analyze the migration and evolution of Lianggaoshan lake-basin. The sedimentary period corresponding to MFS results in widespread distribution of lacustrine mudstone/shale. This widely distributed set of lacustrine mudstone/shale is prone to forming continuous strong reflection coaxial lines on seismic sections, often serving as a marker layer that can be traced throughout the entire study area. In the presence of a lower hyperplane, the lower hyperplane serves as the

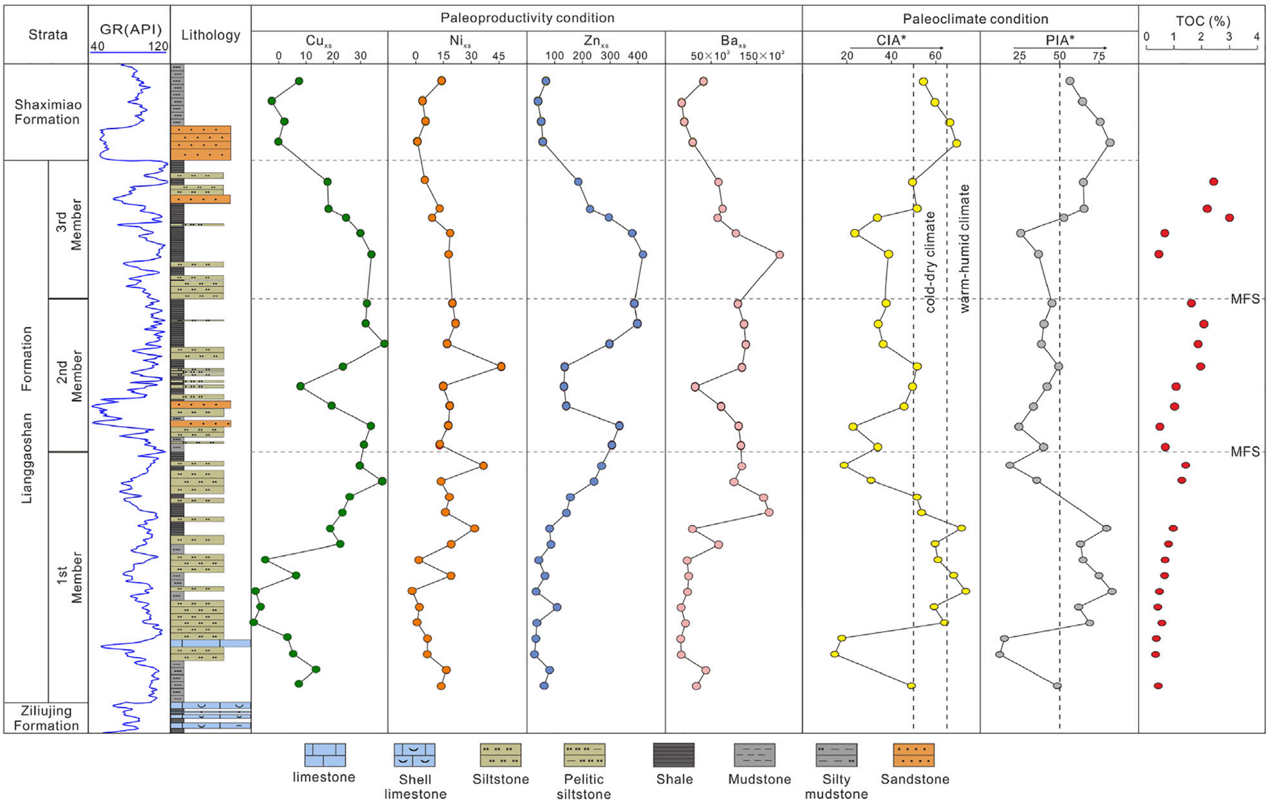

FIGURE 9
Paleoproductivity condition and paleoclimate for the Lianggaoshan Formation.

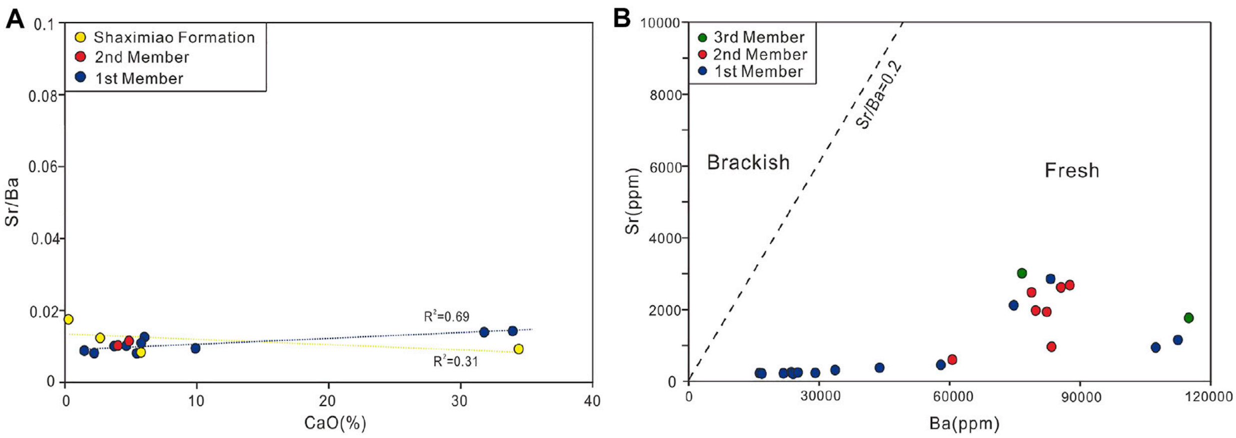

FIGURE 10
(A) Cross-plot of Sr/Ba ratios and CaO concentration for Lianggaoshan lacustrine shale. **(B)** Cross-plot of Ba content and Sr content for Lianggaoshan lacustrine shale.

MFS; in the absence of a undersurface, the MFS can be determined based on the characteristics of the farthest point of the undersurface or strong reflection on the seismic sections. The seismic response characteristics of the MFS inside the Lianggaoshan Fm. are obvious. Affected by the high-speed sandstone at the top, the mudstone/shale at the top of the MFS exhibits continuous and stable strong trough reflections. Figure 5 shows that the MFS of the two periods formed continuous strong reflections on the seismic section, which can be

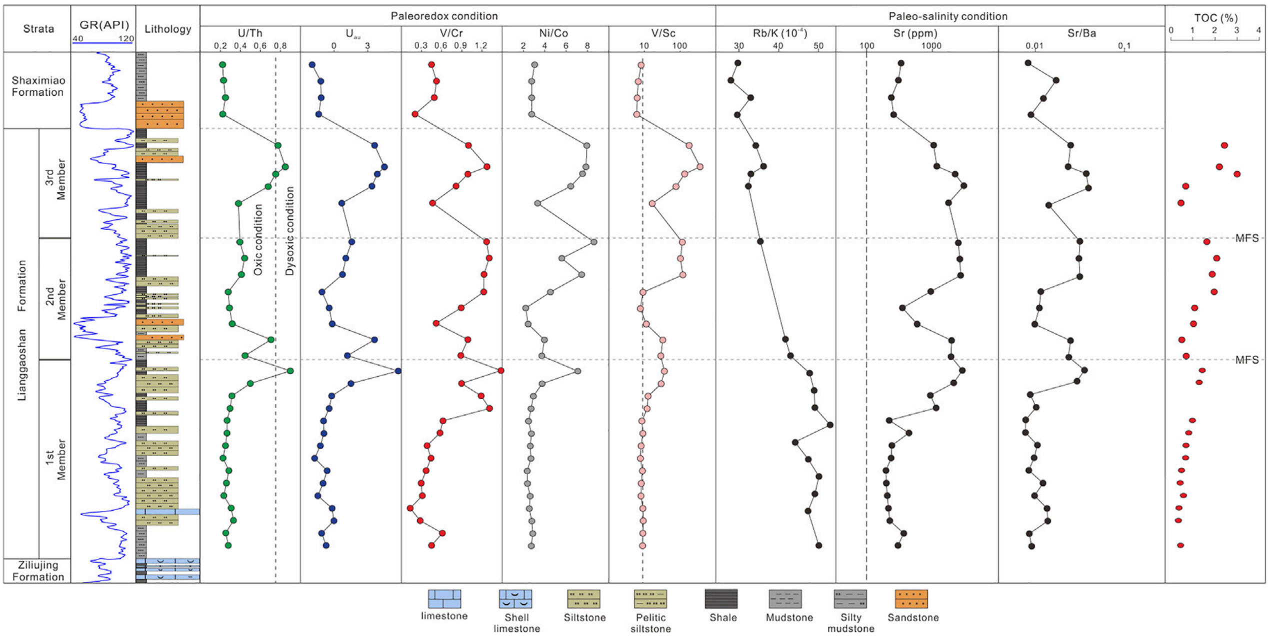

FIGURE 11
Paleoredox condition and paleo-salinity for the Lianggaoshan Formation.

continuously compared and traced in Central, Northern, and Eastern Sichuan Basin. These MFSs are characterized by onlaping sequence boundary (SB) between Lianggaoshan and Ziliujing Formation.

This study utilized the classification method of lacustrine organic-rich shale proposed by Lu et al. (2012). In the TOC range of less than 0.75%, the S_1 value of lacustrine shale is in the low range. As the TOC content increases, S_1 rapidly increases, suggesting that the oil content is rapidly increasing and entering the median range. Subsequently, when the TOC content exceeds 2%, the oil content of Lianggaoshan shale reaches saturation, and the S_1 value reaches equilibrium and hardly rises, entering the high value stage (Figure 6A). Therefore, the TOC lower limit value of Lianggaoshan lacustrine organic-rich shale is 0.75%. Based on the identification and classification criteria of continuous thickness greater than 3 m and logging TOC greater than 0.75% (Figure 6B), the organic-rich shale thickness and spatial distribution in each member of the Liangshan Formation are tracked and compared horizontally.

The spatial distribution characteristics of Lianggaoshan organic-rich shale suggest that six stages of shale are developed from bottom to top (Figure 7), representing multiple migration stages of Lianggaoshan lake-basin. Within Lianggaoshan Fm., the lake-basin within 1st Member formed the 1st to 3rd stage shale, and the depocenter of the lake-basin gradually expanded from the Southeastern to the Central Sichuan Basin (Figure 8A). The lake-basin within 2nd and 3rd Member formed the 4th to 6th stage shale (Figure 7). At this time, the depocenter of the lake-basin is located in the Central Sichuan Basin (Figure 8B). Shale thickness corresponding to MFS of 1st Member reaches maximum in Southeastern Sichuan Basin, with a thickness of 18 m. The depocenter of the lake-basin at the MFS of 2nd Member is near Central Sichuan Basin, with a maximum shale thickness of 14 m (Figure 8B). The organic-rich shale thickness corresponding to the upper 3rd Member is relatively thin (Figure 8C), with a maximum of about 7 m, but the distribution range is relatively large (Figure 8D).

Environmental conditions

Paleo-productivity proxies

The content of life elements (P, Ba, Mo, Cu, Zn, Ni, etc.) can be used as indicators of paleo-productivity (Schoepfer et al., 2015; Gu et al., 2022a; Lei et al., 2023). The selection of paleo-productivity indicators can not only promote plankton development, but also be less susceptible to diagenesis, debris input, and water redox conditions, or can distinguish and correct these effects. Previously, P and Ba were commonly used to reflect the primary productivity of lake water bodies (Deng et al., 2019; Qiu et al., 2022). However, reducing the environment can hinder the accumulation of P and Ba and affect the accuracy of paleo-productivity assessment based on the content of these elements. To avoid the impact of terrigenous debris, $Element_{xs}$ (Cu_{xs}, Ni_{xs}, Zn_{xs}, and Ba_{xs}) can be applied as an indicator of paleo-productivity in lacustrine sediments (Lei et al., 2023). From the trend of vertical variation of TOC, organic-rich shale is developed between the upper part of the 1st and 2nd Member and MFS. Within these intervals (Figure 9), the paleo-productivity indicators (Cu_{xs}, Ni_{xs}, Zn_{xs}, and Ba_{xs}) increase dsignificantly, indicating that the increase in paleo-productivity exhibits positive effects on organic matter enrichment. The upper 3rd Member also develops organic-rich shale, but the paleo-

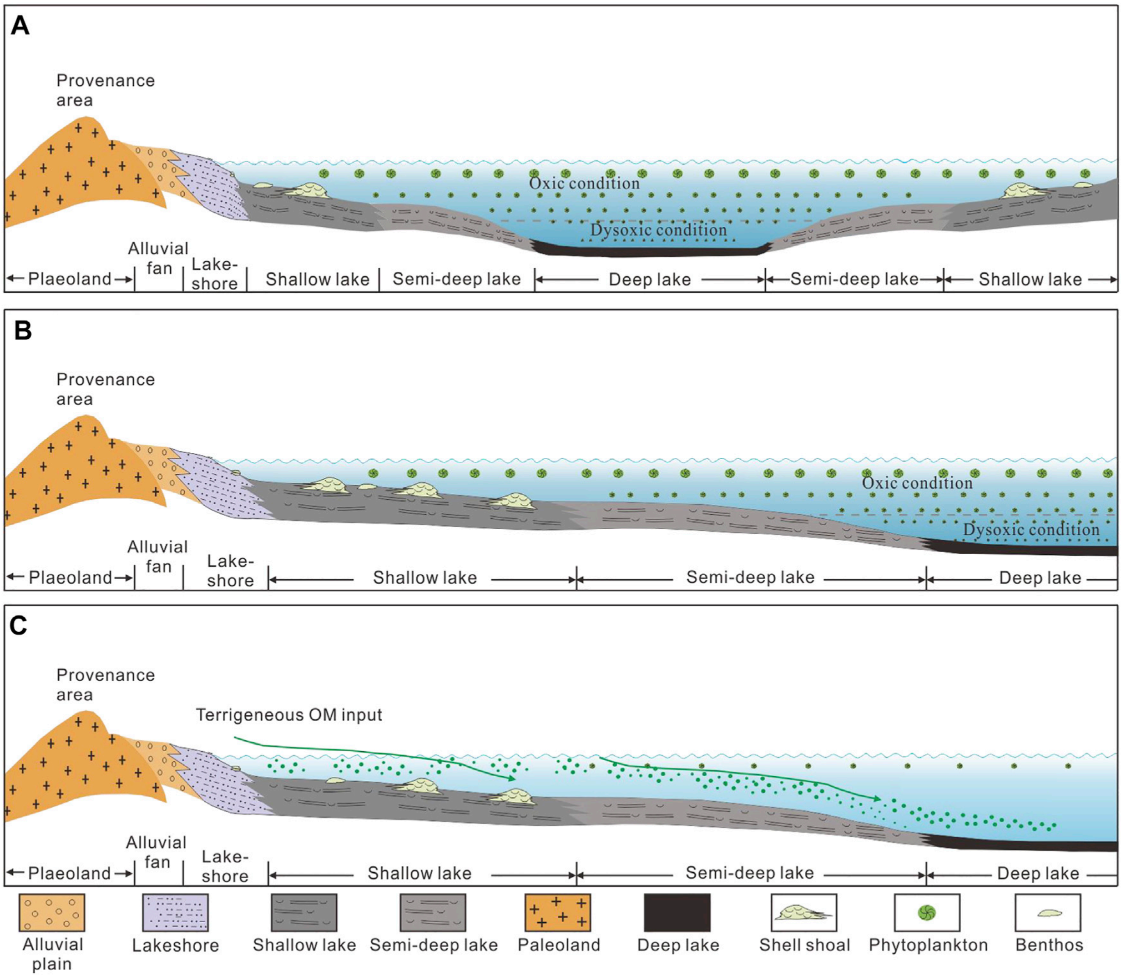

FIGURE 12
Pattern diagram of organic matter enrichment process for the Lianggaoshan Formation. **(A)** 1st Member of Lianggaoshan Formation. **(B)** 2nd Member of Lianggaoshan Formation. **(C)** 3rd Member of Lianggaoshan Formation.

productivity does not have a significant control over the enrichment of organic matter in this interval (Figure 9).

Paleo-climate condition

Climate influences the sedimentary characteristics and organic matter accumulation within the lake-basin by controlling exogenic processes and controlling input of terrestrial sediments. CIA* (Chemical Index of Alteration) and PIA* are classic indicators for assessing paleo-climate (Price et al., 2003; Deng et al., 2019). Higher CIA* and PIA* generally indicate a humid climate, which is conducive to the input of terrigenous debris dominated by weathering (Nesbitt and Young, 1982). The CIA* value for upper part of 1st and 2nd Member is lower than 50, suggesting very low chemical weathering degree (Bai et al., 2015). The CIA* value for upper part of the 3rd Member is between 50 and 65 (Figure 9), suggesting a relatively low chemical weathering degree (Bai et al., 2015). It appears that the paleo-climate of upper part of 3rd Member is more conducive to the input of terrestrial debris than 1st and 2nd Member. The longitudinal variation trend of PIA* exhibits similarity to that of CIA*, reflecting the same characteristics of climate change.

Paleoredox condition

The redox level of bottom water is a key factor in the burial and preservation of OM, and paleoredox-sensitive elements (Mo, U, Ni, V, Cu, Mn, etc.) are commonly used in the reconstruction of paleoredox conditions in lacustrine environments (Algeo and Liu, 2020; Bennett and Canfield, 2020; Algeo and Rowe, 2021). This study used the bimetallic ratio to evaluate the redox condition of lacustrine bottom water. Results indicate that compared to other intervals, the reducibility of the organic-rich interval is significantly stronger. V/Cr, Ni/Co, and V/Sc exhibit high values within the organic-rich interval. The value of U/Th is distributed within the dysoxic condition range within the organic-rich interval. It is suggested that the upper parts of 1st, 2nd and 3rd Member are deposited in a dysoxic condition that is favorable for OM preservation.

Paleosalinity

Ba and Sr were proved to be two indicator elements sensitive to paleosalinity (Deng et al., 2019; Gu et al., 2022a; Gu et al., 2022b). Before using Sr/Ba to evaluate paleosalinity, it is first necessary to remove the adverse effects of carbonate rocks on the data (Gu et al., 2022a; Gu et al., 2022b). The test results of Lianggaoshan lacustrine shale indicate that the vast majority of samples have a CaO content below 10%, which can exclude the interference of carbonate rocks on paleosalinity characterization (Figure 10A). During Lianggaoshan deposition, the paleo-salinity of lake water tends to be freshwater (Figure 10B). However, Sr/Ba ratios significantly increase in the range of organic rich shale, suggesting that an increase in paleo-salinity is beneficial for improving paleo-productivity and thus for enrichment of OM (Figure 11).

Factors of lacustrine organic matter enrichment

During the 1st Member of Lianggaoshan, high biological productivity provided a material basis for lacustrine organic-rich shale (Figure 12A). After formation, the OM immediately entered the burial process. Only when the rate of OM accumulation exceeds the decomposition rate can OM enrichment be caused (Burdige, 2007; Lash and Blood, 2014; Lei et al., 2023). Although the lake-basin is relatively close to the provenance area during 1st Member deposition, but the paleo-climate during this period was not conducive to terrestrial OM input, but due to the large-scale lake-level rise, a dysoxic condition favorable for the preservation of OM was formed at the lake-basin bottom. With the uplift of Dabashan, the distance between the lake basin and the source area becomes farther, which is not conducive to the input of terrestrial OM during 2nd Member deposition. The other conditions controlling OM enrichment in 2nd Member are the same as those of the 1st Member (Figure 12B). During the 3rd Member, paleo-productivity was unable to form a large amount of lacustrine OM. The distance between the lake-basin and the provenance area is also unfavorable for terrestrial OM input. However, due to the favorable paleo-climate for chemical weathering during this period, a large amount of terrestrial organic matter entered the lake-basin (Figure 12C), and a high sedimentation rate can also shorten the time for OM to be oxidized in lake-basin, allowing for rapid deposition and burial of OM, which can also form a dysoxic condition conducive to OM preservation.

Conclusion

1) During Lianggaoshan Fm. deposition, the lake-basin underwent multiple migrations. The multiple migrations of the lake-basin formed six stages of organic-rich shale from bottom to top within the Lianggaoshan Formation. During the deposition of Lianggaoshan Fm. 1st Member, the depocenter of the lake-basin gradually expanded from the southeastern Sichuan Basin to the Central Sichuan Basin. During the deposition of 2nd and 3rd Members, the depocenter of the lake-basin is located in the Central Sichuan Basin. The migration process of depocenters controls the planar distribution of lacustrine organic-rich shale.
2) The Lianggaoshan lacustrine organic-rich shale is distributed from the upper to the top of each member. The OM enrichment during the upper to the top of 1st Member and 2nd Member is controlled by relatively high paleo-productivity and preservation under dysoxic conditions. Organic matter enrichment during upper 3rd Member deposition is controlled by terrestrial input and dysoxic conditions. The dysoxic conditions corresponding to the upper 1st-2nd Member are caused by lake-level rise, while the dysoxic conditions corresponding to the upper 3rd Member are caused by rapid burial.

Data availability statement

The raw data supporting the conclusion of this article will be made available by the authors, without undue reservation.

Author contributions

RF contributed as the major author of the paper. SS, YJ, and DD conceived the project. YaL contributed as rock sample collectors. LQ, QL, and ZJ are responsible for analyzing the data measured in these experiments. All authors contributed to the article and approved the submitted version.

Funding

The research was supported by the National Natural Science Foundation of China (Grant No. 42272171) and Science and Technology Cooperation Program of CNPC–SWPU Innovation Alliance (Grant No. 2020CX020104).

Conflict of interest

Authors RF and YJ were employed by PetroChina Key Laboratory of Unconventional Oil and Gas Resources. Authors SS and DD were employed by PetroChina Research Institute of Petroleum Exploration and Development. Author YaL was employed by Southwest Geophysical Exploration Branch of China Petroleum Group Dongfang Geophysical Exploration Co., Ltd. Authors LQ and QL were employed by CNPC Chuanqing Drilling Engineering Co., Ltd. Author YuL was employed by PetroChina Southwest Oil and Gas Field Company. Author ZJ was employed by Sichuan Geotech Science and Technology Ltd., Company.

Publisher's note

References

Algeo, T. J., and Liu, J. (2020). A re-assessment of elemental proxies for paleoredox analysis. *Chem. Geol.* 540, 119549. doi:10.1016/j.chemgeo.2020.119549

Algeo, T. J., and Rowe, H. (2021). Paleoceanographic applications of trace-metal concentration data. *Chem. Geol.* 324–325, 6–18. doi:10.1016/j.chemgeo.2011.09.002

Bai, H., Yang, X., Xiong, Y., Guan, X., Xu, X., Si, G., et al. (2022). Determination of Lianggaoshan Formation lake strandline and favorable tight oil and gas areas in the central Sichuan Basin. *Nat. Gas. Ind.* 42 (2), 40–49. doi:10.3787/j.issn.1000-0976.2022.02.005

Bai, Y., Liu, Z., Sun, P., Liu, R., Hu, X., Zhao, H., et al. (2015). Rare Earth and major element geochemistry of Eocene fine-grained sediments in oil shale- and coal-bearing layers of the Meihe Basin, Northeast China. *J. Asian Earth Sci.* 97 (97), 89–101. doi:10.1016/j.jseaes.2014.10.008

Bennett, W. W., and Canfield, D. E. (2020). Redox-sensitive trace metals as paleoredox proxies: A review and analysis of data from modern sediments. *Earth Sci. Rev.* 204, 103175. doi:10.1016/j.earscirev.2020.103175

Burdige, D. J. (2007). Preservation of organic matter in marine sediments: Controls, mechanisms, and an imbalance in sediment organic carbon budgets? *Chem. Rev.* 107, 467–485. doi:10.1021/cr050347q

Cai, G., Gu, Y., Fu, Y., Jiang, Y., Wei, Z., Wang, Z., et al. (2023). Pore system classification of Jurassic Da'anzhai Member lacustrine shale: Insight from pore fluid distribution. *Energy Explor. Exploitation* 41 (3), 900–921. doi:10.1177/01445987231154613

Cheng, D., Zhang, Z., Hong, H., Zhang, S., Qin, C., Yuan, X., et al. (2023). Sedimentation and provenance and the basin-mountain relationship of the jurassic Lianggaoshan Formation in eastern Sichuan Basin. SW China. *Petroleum Explor. Dev.* 50 (2), 262–272. doi:10.11698/PED.20220412

Deng, T., Li, Y., Wang, Z. J., Yu, Q., Dong, S., Yan, L., et al. (2019). Geochemical characteristics and organic matter enrichment mechanism of black shale in the Upper Triassic Xujiahe Formation in the Sichuan basin: Implications for paleoweathering, provenance and tectonic setting. *Mar. Petroleum Geol.* 109, 698–716. doi:10.1016/j.marpetgeo.2019.06.057

Fu, Y., Jiang, Y., Dong, D., Hu, Q., Lei, Z., Peng, H., et al. (2021). Microscopic pore-fracture configuration and gas-filled mechanism of shale reservoirs in the Western Chongqing area, Sichuan Basin,China. *Petroleum Explor. Dev.* 48 (5), 1063–1076. doi:10.1016/s1876-3804(21)60091-5

Fu, Y., Jiang, Y., Wang, Z., Hu, Q., Xie, J., Ni, G., et al. (2019). Non-connected pores of the longmaxi shale in southern Sichuan Basin of China. *Mar. Petroleum Geol.* 110, 420–433. doi:10.1016/j.marpetgeo.2019.07.014

Gu, Y., Hu, D., Wei, Z., Liu, R., Hao, J., Han, J., et al. (2022b). Sedimentology and geochemistry of the upper permian linghao formation marine shale, central nanpanjiang basin, SW China. *Front. Earth Sci.* 10, 914426. doi:10.3389/feart.2022.914426

Gu, Y., Li, X., Qi, L., Li, S., Jiang, Y., Fu, Y., et al. (2022a). Sedimentology and geochemistry of the lower permian shanxi formation Shan 2^3 submember transitional shale, eastern ordos basin, north China. *Front. Earth Sci.* 10, 859845. doi:10.3389/feart.2022.859845

He, W., He, H., Wang, Y., Cui, B., Meng, Q., Guo, X., et al. (2022). Major breakthrough and significance of shale oil of the jurassic Lianggaoshan Formation in well ping'an 1 in northeastern Sichuan Basin. *China Pet. Explor.* 27 (1), 40–49. doi:10.3969/j.issn.1672-7703.2022.01.004

Hu, D., Li, Z., Wei, Z., Duan, J., Miao, Z., Pan, L., et al. (2023). Breakthrough in oil and gas exploration of Jurassic channel sandstone in Well Bazhong 1HF in northern Sichuan Basin and its significance. *Nat. Gas. Ind.* 43 (3), 1–11. doi:10.3787/j.issn.1000-0976.2023.03.001

Hu, D., Wei, Z., Liu, R., Wei, X., Chen, F., and Liu, Z. (2021a). Enrichment control factors and exploration potential of lacustrine shale oil and gas: A case study of jurassic in the fuling area of the Sichuan Basin. *Nat. Gas. Ind.* 41 (8), 1–8. doi:10.1016/j.ngib.2021.08.012

Hu, Z., Wang, R., Liu, Z., Liu, G., Feng, D., Yang, Z., et al. (2021b). Lin28a is essential for synaptic plasticity in dentate granule cells and spatial memory. *Earth Sci. Front.* 1, 261–266. doi:10.1007/s12264-020-00591-7

Huang, D. (2019). Jurassic integrative stratigraphy and timescale of China. *Sci. China Earth Sci.* 62 (1), 223–255. doi:10.1007/s11430-017-9268-7

Jiang, C., Zhang, H., Zhou, Y., Gan, H., Pu, J., Jiang, Y., et al. (2022). Paleogeomorphic characteristics of wufeng—longmaxi formation and its influence on development of high-quality shale in dazu area, Western chongqing. *J. Central South Univ. Technol.* 53 (9), 3628–3640. doi:10.11817/j.issn.1672-7207.2022.09.026

Lai, Q., Qi, L., Chen, S., Ma, S., Zhou, Y., Fang, P., et al. (2023). Resercoir space characteristics and pore structure of Jurassic Lianggaoshan Formation lacustrine shale reservoir in Sichuan Basin, China: Insights into controlling factors. *Front. Earth Sci.* 11, 1133413. doi:10.3389/feart.2023.1133413

Lash, G. G., and Blood, D. R. (2014). Organic matter accumulation, redox, and diagenetic history of the Marcellus Formation, southwestern Pennsylvania, Appalachian basin. *Mar. Petroleum Geol.* 57, 244–263. doi:10.1016/j.marpetgeo.2014.06.001

Lei, W., Chen, D., Liu, Z., and Cheng, M. (2023). Paleoenvironment-driven organic matter accumulation in lacustrine shale mixed with shell bioclasts:A case study from the Jurassic Da'anzhai member, Sichuan Basin (China). *J. Petroleum Sci. Eng.* 220, 111178. doi:10.1016/j.petrol.2022.111178

Li, J., Li, H., Yang, C., Ren, X. H., and Li, Y. D. (2023). Geological characteristics of deep shale gas and their effects on shale fracability in the Wufeng–Longmaxi Formations of the southern Sichuan Basin, China. *Lithosphere* 1, 4936993. doi:10.2113/2023/4936993

Li, J., Li, H., Yang, C., Wu, Y. J., Gao, Z., and Jiang, S. L. (2022). Geological characteristics and controlling factors of deep shale gas enrichment of the Wufeng-Longmaxi Formation in the southern Sichuan Basin, China. *Lithosphere 2022* S12, 4737801. doi:10.2113/1970/4737801

Liang, H., Xu, G., Xu, F., Yu, Q., Liang, J., and Wang, D. (2020). Paleoenvironmental evolution and organic matter accumulation in an oxygen-enriched lacustrine basin: A case study from the laizhou bay sag, southern bohai sea (China). *Int. J. Coal Geol.* 217, 103318. doi:10.1016/j.coal.2019.103318

Liu, J., Cao, J., Hu, G., Wang, Y., Yang, R., and Liao, Z. (2020). Water-level and redox fluctuations in a Sichuan Basin lacustrine system coincident with the Toarcian OAE. *Palaeogeogr. Palaeoclimatol. Palaeoecol.* 558, 109942. doi:10.1016/j.palaeo.2020.109942

Lu, S., Huang, W., Chen, F., Li, J., Wang, Min., Xue, Haitao., et al. (2012). Classification and evaluation criteria of shale oil and gas resources:Discussion and application. *Petroleum Explor. Dev.* 39 (2), 268–276. doi:10.1016/s1876-3804(12)60042-1

Murphy, A. E., Sageman, B. B., Hollander, D. J., Lyons, T. W., and Brett, C. E. (2000). Black shale deposition and faunal overturn in the devonian appalachian basin: Clastic starvation, seasonal water-column mixing, and efficient biolimiting nutrient recycling. *Paleoceanography* 15, 280–291. doi:10.1029/1999PA000445

Nesbitt, H., and Young, G. (1982). Early proterozoic climates and plate motions inferred from major element chemistry of lutites. *Nature* 299 (5885), 715–717. doi:10.1038/299715a0

Price, J. R., and Velbel, M. A. (2003). Chemical weathering indices applied to weathering profiles developed on heterogeneous felsic metamorphic parent rocks. *Chem. Geol.* 202, 397–416. doi:10.1016/j.chemgeo.2002.11.001

Qiu, Z., and He, J. (2022). Depositional environment changes and organic matter accumulation of Pliensbachian-Toarcian lacustrine shales in the Sichuan basin, SW China. *J. Asian Earth Sci.* 232, 105035. doi:10.1016/j.jseaes.2021.105035

Qiu, Z., and Zou, C. (2020a). Controlling factors on the formation and distribution of "sweet-spot areas" of marine gas shales in South China and a preliminary discussion on unconventional petroleum sedimentology. *J. Asian Earth Sci.* 194, 103989. doi:10.1016/j.jseaes.2019.103989

Qiu, Z., and Zou, C. (2020b). Unconventional petroleum sedimentology: Connotation and prospect. *Acta Sedimentol. Sin.* 38, 1–29. doi:10.14027/j.issn.1000●0550.2019.116

Ross, D. J. K., and Bustin, R. M. (2009). The importance of shale composition and pore structure upon gas storage potential of shale gas reservoirs. *Mar. Petroleum Geol.* 26, 916–927. doi:10.1016/j.marpetgeo.2008.06.004

Schoepfer, S. D., Shen, J., Wei, H., Tyson, R. V., Ingall, E., and Algeo, T. J. (2015). Total organic carbon, organic phosphorus, and biogenic barium fluxes as proxies for paleomarine productivity. *Earth Sci. Rev.* 149, 23–52. doi:10.1016/j.earscirev.2014.08.017

Tribovillard, N., Algeo, T. J., Lyons, T., and Riboulleau, A. (2006). Trace metals as paleoredox and paleoproductivity proxies: An update. *Chem. Geol.* 232 (1/2), 12–32. doi:10.1016/j.chemgeo.2006.02.012

Wang, R., Ding, W., Zhang, Y., Wang, Z., Wang, X., He, J., et al. (2016b). Analysis of developmental characteristics and dominant factors of fractures in lower cambrian marine shale reservoirs: A case study of niutitang formation in cen'gong block, southern China. *J. Petroleum Sci. Eng.* 138, 31–49. doi:10.1016/j.petrol.2015.12.004

Wang, R., Gu, Y., Ding, W., Gong, D., Yin, S., Wang, X., et al. (2016a). Characteristics and dominant controlling factors of organic-rich marine shales with high thermal maturity: A case study of the lower cambrian niutitang formation in the cen'gong block, southern China. *J. Nat. Gas Sci. Eng.* 33, 81–96. doi:10.1016/j.jngse.2016.05.009

Wang, R., Hu, Z., Sun, C., Liu, Z., Zhang, C., Gao, B., et al. (2018). Comparative analysis of shale reservoir characteristics in the wufeng-longmaxi (O_3w-S_1l) and niutitang ($Є_1$n) formations: A case study of the wells JY1 and TX1 in southeastern Sichuan Basin and its periphery, SW China. *Interpretation* 6 (4), SN31–SN45. doi:10.1190/int-2018-0024.1

Zou, C., Zhang, G., Yang, Z., Tao, S., Hou, L., Zhu, R., et al. (2013). Geological concepts, characteristics, resource potential and key techniques of unconventional hydrocarbon: On unconventional petroleum geology. *Petroleum Explor. Dev.* 40 (4), 385–399. doi:10.11698/PED.2013.04.01

Zou, C., Zhu, R., Chen, Z., Ogg, J. G., Wu, S., Dong, D., et al. (2019). Organic-matter-rich shales of China. *Earth Sci. Rev.* 189, 51–78. doi:10.1016/j.earscirev.2018.12.002